 SDHM, vol.5, no.1, pp.57-72, 2009

An Automated Procedure for the Geometrical Modelling of a Surface Crack Front

J. Toribio[1], J.C. Matos[2], B. González[1] and J. Escuadra[2]

Abstract: In this paper an automatic (analytical-numerical) procedure is proposed to model the front of a transverse surface crack located in the circular section of a lineal structural element (wire, cable, strand, rod, shaft,..., i.e., a cylindrical geometry) by means of a fitting ellipse, obtaining the ellipse parameters from a series of points in the *real* crack front and adjusting them to the *theoretical* fitting ellipse by a least square method. For symmetric cracks two modelling procedures are formulated: (i) in the first one, a fitting ellipse is used wit its centre belonging to the periphery of the circular section of the cylinder; (ii) in the second one, a circle is used with no restrictions regarding the position of its centre. Both methods were compared and applied to real cracks in high-strength steel wires subjected to fatigue.

Keywords: Semi-elliptical surface cracks, round bars, geometrical modelling, crack fronts, fatigue.

1 Introduction

In the field of structural integrity the circular cylinder with a transverse surface crack of semi-elliptical shape is one of the key geometries in engineering fracture mechanics. Such a cracked geometry is representative of a wide set of linear structural elements working in tension such as wire, cables, tendons, strands, shafts, ... subjected to monotonic or cyclic loading, working in an inert or aggressive environment and thus susceptible to suffer subcritical crack growth in the form of fatigue, stress corrosion cracking or corrosion-fatigue.

To model a transverse surface crack an a cylinder, previous researchers have chosen geometrical entities such as lines, circles or ellipses [James and Mills (1988); Carpinteri (1993); Levan and Royer (1993); Couroneau and Royer (2000); Toribio and Toledano (2000); Shin and Cai (2004)], sometimes applying restrictions to fit

[1] Dept. of Materials Engineering, University of Salamanca, Spain
[2] Dept. of Computing Engineering, University of Salamanca, Spain

such geometrical entities to the real shape of the crack. In this framework, the ellipse is the most widely used geometry to model a surface crack front, due to its simplicity and adequacy to most real cases because two only parameters (the crack depth a and the length of the major semiaxis of the ellipse b) are needed to define the crack shape.

In this paper the crack front is modelled by means of elliptical and circular geometries. The analysis was focussed on two cases of special interest: (i) an ellipse with its centre located at the cylinder surface [Carpinteri (1993); Couroneau and Royer (2000); Toribio and Toledano (2000); Shin and Cai (2004)] and (ii) a circle with no restriction regarding the location of its centre [James and Mills (1988); Levan and Royer (1993)].

2 General procedure

The shape of the most general ellipse able to model the crack front has five degrees of freedom $\{a, b, \varphi, \beta, l\}$, as shown in Fig. 1. Variables of analysis will be named $z_1 = a$, $z_2 = b$, ..., $z_5 = l$ throughout this paper. The origin (0,0) of the coordinate axes is located at the centre of the cylinder section. Each elliptical crack front is modelled by means of an ellipse obtained from a set of n points (x_i, y_i).

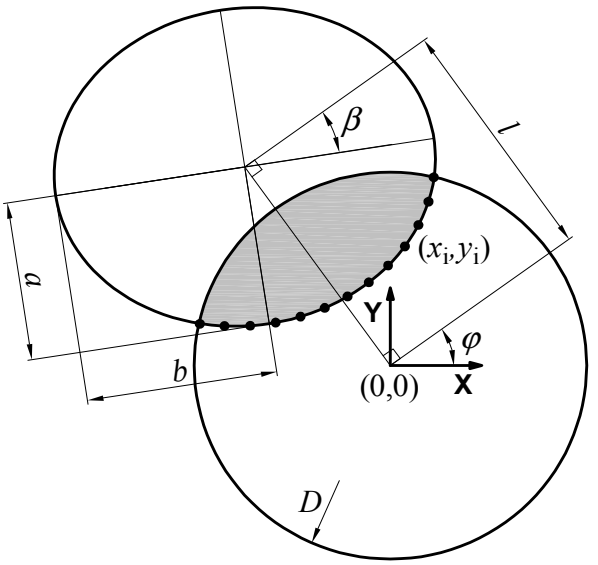

Figure 1: Elliptical modelling of the crack front

The starting point was the choice of the initial parameters z^*, calculated using the

minimum necessary points at the crack front to obtain the initial ellipse. With these values z^* and with the points (x_i, y_i) of the elliptical line, an iterative procedure was used to obtain a difference between consecutive numerical results z lower than a defined error, thus obtaining a set of points (x_i, y_i) fitted to the real crack front. It was an automated procedure in which several numerical programs were assembled using Mathematica®.

The process was based on the minimization of the following function,

$$F(z) = \sum_{i=1}^{n} (\hat{y}_i - y_i)^2 \tag{1}$$

where $\hat{y}_i$ is the coordinate of the ellipse corresponding to the parameters z and the point x_i (i.e., the ellipse of parameters z contains the set of points $(x_i, \hat{y}_i)$).

Using the Taylor series expansion of the function $\partial F/\partial z_k$ at the point z^* with regard to the z variables, and calling R to the remaining points (not considered in the calculation of the optimal curve),

$$\frac{\partial F}{\partial z_k}(z) = \left(\frac{\partial F}{\partial z_k}\right)(z^*) + \sum_j \left((z_j - z_j^*)\left(\frac{\partial^2 F}{\partial z_j \partial z_k}\right)(z^*)\right) + R \tag{2}$$

and applying the minimisation condition,

$$\frac{\partial F}{\partial z_k}(z) = 0 \text{ for } k = 1, \ldots, 5 \tag{3}$$

finally a mathematical expression is obtained so that, using it iteratively, gives the z value to determine the optimal ellipse which best fits the real crack front.

Due to the consideration of only the first terms in the Taylor series expansion, a factor $h \ll 1$ must be introduced to guarantee that the remaining terms can be neglected, the result being,

$$z = z^* - h\left(\frac{\partial^2 F}{\partial z_j \partial z_k}\right)^{-1}(z^*)\left(\frac{\partial F}{\partial z_k}\right)(z^*) \tag{4}$$

and this new value should, theoretically, being nearest to the point at which partial derivatives are zero, so that the iterative procedure is initiated again taking this value as the new z^*.

The described general procedure is very complicated and time consuming when it involves the five variables and it does not significantly improves the quality of numerical results when compared to similar procedures with some restrictions. Therefore, two simplified procedures will be used in this paper, as described in the following sections.

2.1 Non symmetric modelling

In the case of non symmetric cracks the crack front was characterised as an ellipse with its centre located at the cylinder surface, as depicted in Fig. 2. In this modelling the l parameter (distance between the centres of the circular section of the cylinder and the ellipse) is fixed with a value $l = D/2$ (D being the diameter of the cylinder), so that the space of parameters has only four variables, and the variation of the angles β and φ is permitted, thus obtaining the following equation for the ellipse:

$$\frac{(A\cos\beta + B\sin\beta)^2}{b^2} + \frac{(-A\sin\beta + B\cos\beta)^2}{a^2} = 1 \tag{5}$$

To simplify this expression, two additional parameters A and B, being dependent on the angular variable φ, are introduced as:

$$A = x\cos\varphi + y\sin\varphi \tag{6}$$

$$B = -x\sin\varphi + y\cos\varphi - \frac{D}{2} \tag{7}$$

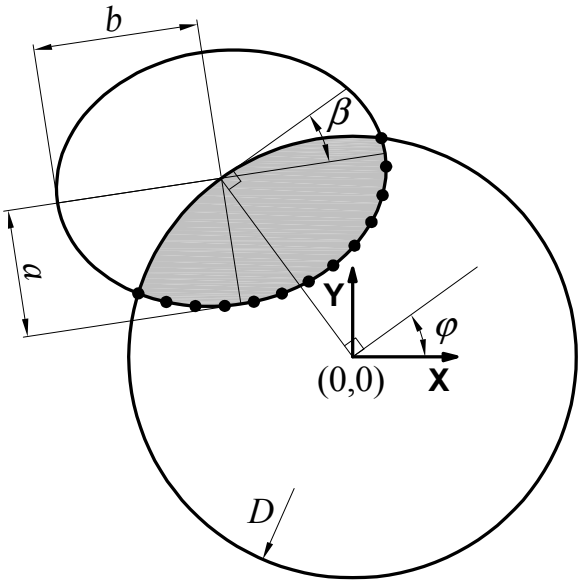

Figure 2: Non symmetrical elliptical modelling of the crack front

In this case the function F to minimize is:

$$\begin{aligned} F = & \left(\left(\left(\frac{D}{2} \right) \left(- \left(a^2 + b^2 \right) \cos \varphi + \left(a^2 - b^2 \right) \cos \left(2\beta + \varphi \right) \right) - \right. \right. \\ & - \sqrt{2} ab \left(-a^2 - b^2 + 2x_i^2 + \left(\frac{D}{2} \right)^2 \left(1 - \cos \left(2\varphi \right) \right) + 2Dx_i \sin \varphi + \right. \\ & + \left(a^2 - b^2 \right) \cos \left(2 \left(\beta + \varphi \right) \right) \Big)^{1/2} + a^2 x_i \sin \left(2 \left(\beta + \varphi \right) \right) - \\ & \left. \left. - b^2 x_i \sin \left(2 \left(\beta + \varphi \right) \right) \right) \left(\frac{-1}{a^2 + b^2 + \left(-a^2 + b^2 \right) \cos (2(\beta + \varphi))} \right) - y_i \right)^2 \end{aligned} \tag{8}$$

including its partial derivatives as:

$$\begin{pmatrix} H_1 \\ H_2 \\ H_3 \\ H_4 \end{pmatrix} = - \sum_{i=1}^{13} \left(\begin{pmatrix} \frac{\partial^2 F}{\partial a^2} & \frac{\partial^2 F}{\partial b \partial a} & \frac{\partial^2 F}{\partial \varphi \partial a} & \frac{\partial^2 F}{\partial \beta \partial a} \\ \frac{\partial^2 F}{\partial a \partial b} & \frac{\partial^2 F}{\partial b^2} & \frac{\partial^2 F}{\partial \varphi \partial b} & \frac{\partial^2 F}{\partial \beta \partial b} \\ \frac{\partial^2 F}{\partial a \partial \varphi} & \frac{\partial^2 F}{\partial b \partial \varphi} & \frac{\partial^2 F}{\partial \varphi^2} & \frac{\partial^2 F}{\partial \beta \partial \varphi} \\ \frac{\partial^2 F}{\partial a \partial \beta} & \frac{\partial^2 F}{\partial b \partial \beta} & \frac{\partial^2 F}{\partial \varphi \partial \beta} & \frac{\partial^2 F}{\partial \beta^2} \end{pmatrix}^{-1} \right)_z \begin{pmatrix} \frac{\partial F}{\partial a} \\ \frac{\partial F}{\partial b} \\ \frac{\partial F}{\partial \varphi} \\ \frac{\partial F}{\partial \beta} \end{pmatrix}_z \tag{9}$$

where i indicates each of the points considered in the calculation and the subindex z indicates the point where the partial derivatives are evaluated.

The process is repeated iteratively, introducing at each step the result obtained in the previous one up to the moment in which the new values of $\{a, b, \varphi, \beta\}$ differ from the previous ones in values lower than $\{H_1, H_2, H_3, H_4\}$, these being the admitted tolerances (taken as 0.001 in this paper), i.e.,

$$\left| a' - a \right| < H_1 \tag{10}$$

$$\left| b' - b \right| < H_2 \tag{11}$$

$$\left| \varphi' - \varphi \right| < H_3 \tag{12}$$

$$\left| \beta' - \beta \right| < H_4 \tag{13}$$

$(a', b', \varphi', \beta')$ being the new point obtained from (a, b, φ, β).

2.2 Symmetric modelling

This method implies the restriction of considering a symmetric crack, and thus the centre of the cylinder circular section is contained in the prolonged axis of the ellipse (Fig. 3). The variables $\{a, b, l, \varphi\}$ considered in this method are related by the following expression:

$$\frac{(x \cos \varphi + y \sin \varphi)^2}{b^2} + \frac{(-x \sin \varphi + y \cos \varphi - l)^2}{a^2} = 1 \tag{14}$$

In spite of the fact that this method provides a more exact solution for symmetric cracks, it is still very complicated with no clear advantages in the matter of accuracy. Therefore, an additional restriction will be imposed in the procedure to have a simpler, flexible and accurate fitting procedure.

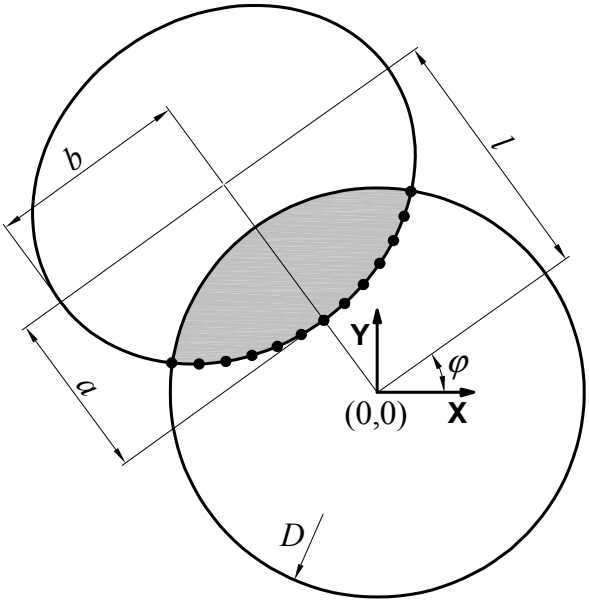

Figure 3: Symmetrical elliptical modelling of the crack front

2.2.1 *Elliptical symmetrical modelling with its centre at the cylinder surface*

In this case the crack front is modelled as a symmetrical ellipse with its centre located at the cylinder surface, thus fixing the l parameter (of the value $D/2$), as shown in Fig. 4. The parameters defining the crack front in this modelling are the dimensionless crack depth a/D, the aspect ratio a/b and the angle φ. The three degrees of freedom characterising this ellipse are $\{a, b, \varphi\}$, they being related by the following expression:

$$\frac{(x\cos\varphi + y\sin\varphi)^2}{b^2} + \frac{\left(-x\sin\varphi + y\cos\varphi - \frac{D}{2}\right)^2}{a^2} = 1 \tag{15}$$

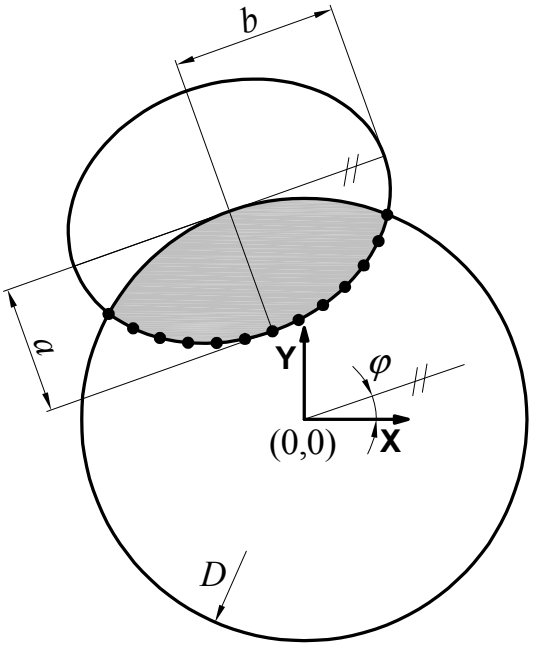

Figure 4: Symmetrical modelling of the crack front by means of an ellipse with its centre located at the cylinder surface

The function F to minimize is:

$$\begin{aligned} F = \Bigg(& \frac{1}{2\left(b^2\cos^2\varphi + a^2\sin^2\varphi\right)}\left(b^2 D\cos\varphi + \right. \\ & + \sqrt{2}ab\left(-a^2 - b^2 + \frac{D^2}{4} + 2x_i^2 + \left(a^2 - b^2 - \frac{D^2}{4}\right)\cos(2\varphi) + \right. \\ & \left. \left. + 2Dx_i\sin\varphi\right)^{1/2} - a^2 x_i\sin(2\varphi) + b^2 x_i\sin(2\varphi)\right) - y_i\Big)^2 \end{aligned} \tag{16}$$

and the equation to solve is:

$$\begin{pmatrix} H_1 \\ H_2 \\ H_3 \end{pmatrix} = -\sum_{i=1}^{13} \left(\begin{pmatrix} \frac{\partial^2 F}{\partial a^2} & \frac{\partial^2 F}{\partial b \partial a} & \frac{\partial^2 F}{\partial \varphi \partial a} \\ \frac{\partial^2 F}{\partial a \partial b} & \frac{\partial^2 F}{\partial b^2} & \frac{\partial^2 F}{\partial \varphi \partial b} \\ \frac{\partial^2 F}{\partial a \partial \varphi} & \frac{\partial^2 F}{\partial b \partial \varphi} & \frac{\partial^2 F}{\partial \varphi^2} \end{pmatrix}^{-1} \right)_z \begin{pmatrix} \frac{\partial F}{\partial a} \\ \frac{\partial F}{\partial b} \\ \frac{\partial F}{\partial \varphi} \end{pmatrix}_z \tag{17}$$

The result of each iteration feeds the input of the procedure up to the instant in which the values of $\{a, b, \varphi\}$ differ from those introduced in $\{H_1, H_2, H_3\}$ in a

value lower that the tolerance (fixed as 0.001 in this paper), i.e.:

$$\left|a' - a\right| < H_1 \tag{18}$$

$$\left|b' - b\right| < H_2 \tag{19}$$

$$\left|\varphi' - \varphi\right| < H_3 \tag{20}$$

2.2.2 Circumpherential modelling

The crack front is represented by a circular portion with no restriction at all (Fig. 5), so that the ellopse parameters become only one, the circle radius R_c. The parameters defining the crack front in this modelling are the dimensionless crack depth a/D, the aspect ratio a/R_c and the angle φ. The three degrees of freedom are $\{R_c, l, \varphi\}$, obtaining the following equation for the circle,

$$(x + l\sin\varphi)^2 + (y - l\cos\varphi)^2 = R_c^2 \tag{21}$$

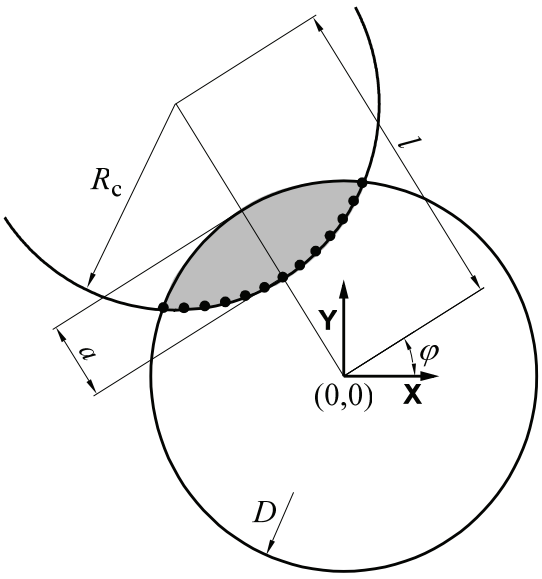

Figure 5: Symmetrical modelling of the crack front by means of a circle with no restrictions regarding its centre

The function F to minimize is:

$$F = \left(\left(l\cos\varphi - \sqrt{R_c^2 - (x_i - l\,\sin\varphi)^2} \right) - y_i \right)^2 \tag{22}$$

where ($x_0 = l\sin\varphi$, $y_0 = l\cos\varphi$) are the coordinates of the circle centre. The equation to solve in this case is:

$$\begin{pmatrix} H_1 \\ H_2 \\ H_3 \end{pmatrix} = -\sum_{i=1}^{13} \left(\begin{pmatrix} \frac{\partial^2 F}{\partial R_c^2} & \frac{\partial^2 F}{\partial l \partial R_c} & \frac{\partial^2 F}{\partial \varphi \partial R_c} \\ \frac{\partial^2 F}{\partial R_c \partial l} & \frac{\partial^2 F}{\partial l^2} & \frac{\partial^2 F}{\partial \varphi \partial l} \\ \frac{\partial^2 F}{\partial R_c \partial \varphi} & \frac{\partial^2 F}{\partial l \partial \varphi} & \frac{\partial^2 F}{\partial \varphi^2} \end{pmatrix}^{-1} \right)_z \begin{pmatrix} \frac{\partial F}{\partial R_c} \\ \frac{\partial F}{\partial l} \\ \frac{\partial F}{\partial \varphi} \end{pmatrix}_z \tag{23}$$

The result of each iteration feeds the input of the procedure up to the instant in which the values of $\{R_c,\ l,\ \varphi\}$ differ from those introduced in $\{H_1,\ H_2,\ H_3\}$ in a value lower that the tolerance (fixed as 0.001 in this paper), i.e.:

$$\left| R_c' - R_c \right| < H_1 \tag{24}$$

$$\left| l' - l \right| < H_2 \tag{25}$$

$$\left| \varphi' - \varphi \right| < H_3 \tag{26}$$

3 Discussion

To compare the accuracy of the two proposed methods to model the geometry of real surface crack fronts in cylinders, an evaluation was made of the function $F(z_i)$, taking the same number of points $(x_i,\ y_i)$ in the modelling of the crack front, and dividing by D^2 to obtain a dimensionless value. The obtained parameter, ξ, was used as en estimator of the mathematical error with each fitting method.

Starting from a initially perfect circular crack front, the error ξ was estimated when the crack front is modelled as an ellipse, for different relations a/D and a/R_c (Fig. 6), using 13 points to represent the circle arch. The aspect ratio a/b is plotted in Fig. 7 against the relative crack depth a/D for different values of a/R_c.

The evolution from a circular to an elliptical crack front can be represented by expressing the aspect ratio a/b as a function of a/R_c (a/D being constant) using a third degree polynomial expression with a regression coefficient of 1.000. A special case is a/R_c = 1.000 in which both fitting procedures coincide, the crack front being a circumpherence with its centre at the cylinder surface.

To check the modelling procedures from the experimental point of view, real fractographs were used showing the crack front shape evolution in high strength steel wires subjected to fatigue (cyclic) loading (Fig. 8). Starting from the modelling

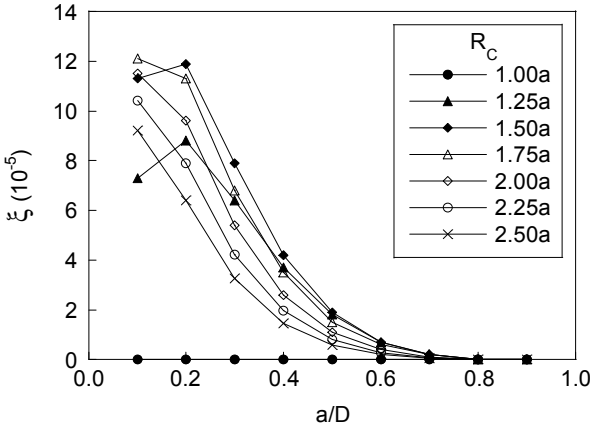

Figure 6: Error parameter, ξ, as a function of the relative crack depth a/D

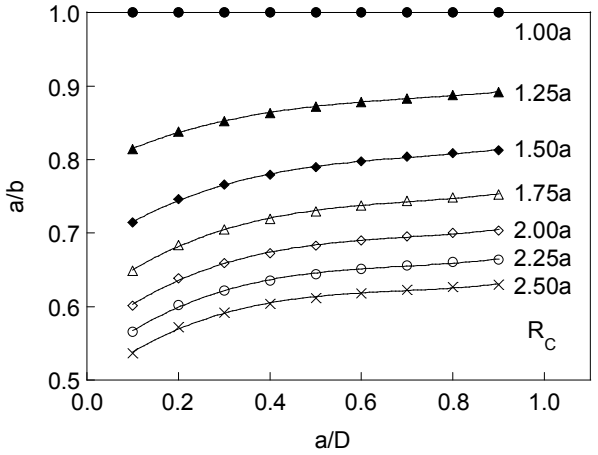

Figure 7: Relationship a/b *vs* a/D, for different values of R_c

of the visible crack fronts (points located at the *real* crack fronts) such lines were modelled with the two procedures of ellipse centred at the cylinder surface and circle with no restriction. The obtained results showed that the computed parameters a and φ are practically the same in both methods, as plotted in Figs. 9-10.

For a unique crack front the angle φ does not have a high interest. However, it is relevant when the *evolution* of the crack front shape has to be analyzed. In this case the parameters R_c and b, characteristic the two modelling procedures, are related

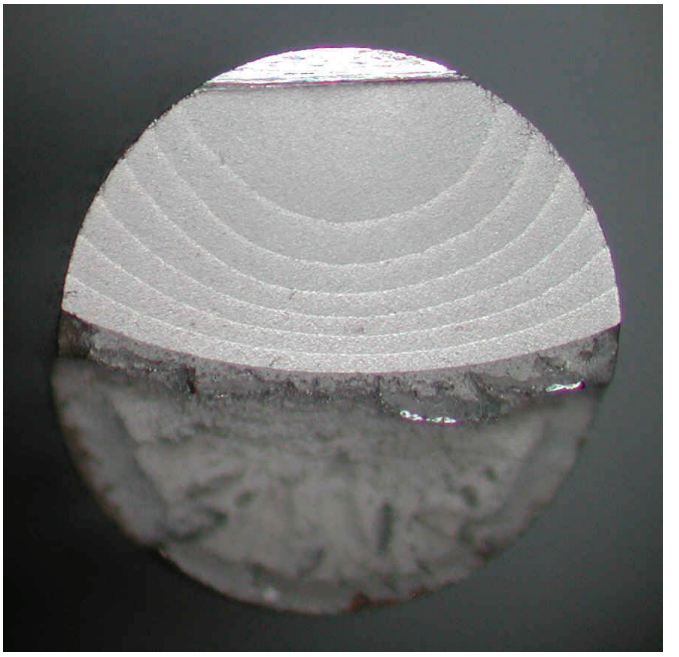

Figure 8: High strength steel wire cracked by fatigue

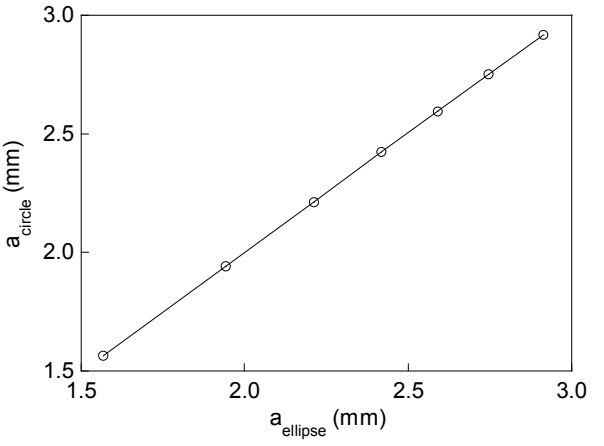

Figure 9: Crack depth obtained by means of the two fitting procedures (ellipse and circle)

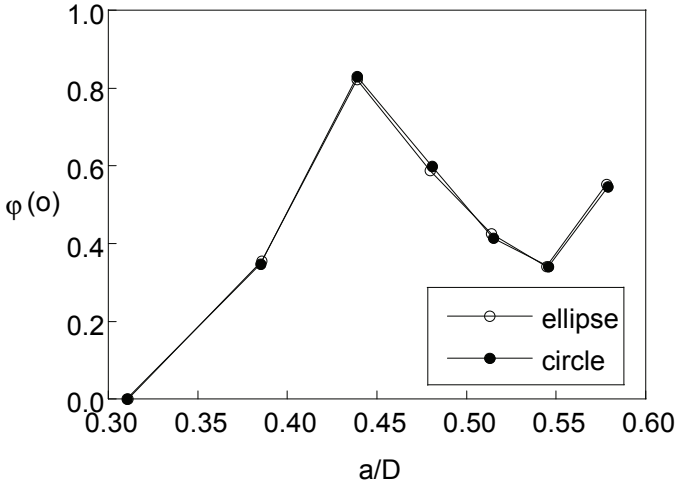

Figure 10: Plot of the φ angle as a function of the relative crack depth (a/D) in the two fitting procedures (ellipse and circle)

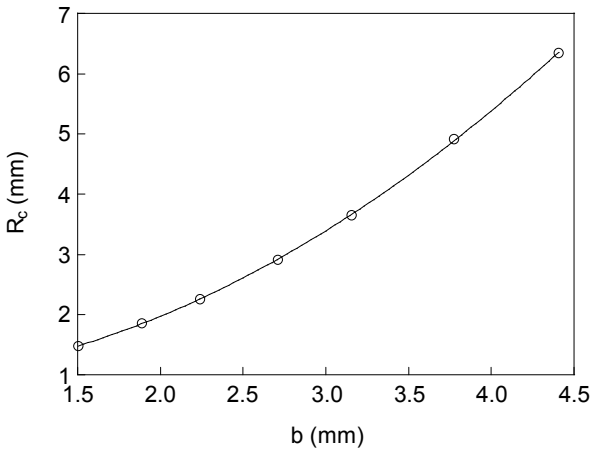

Figure 11: Parameters R_c and b

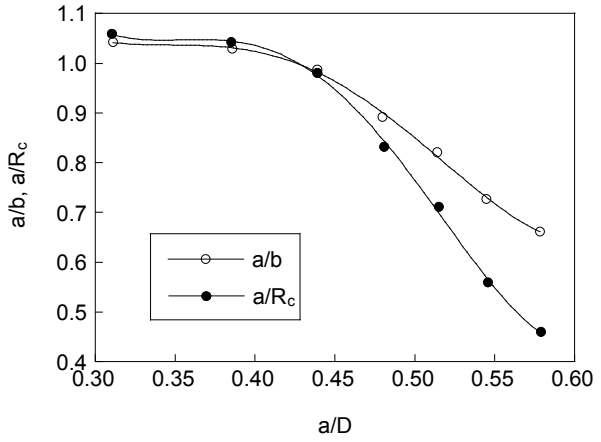

Figure 12: Characteristic dimensionless relations

as shown in Fig. 11, and this relationship may be expressed by means of a second-order polynomial expression with a regression coefficient of 1.000 as:

$$R_c = 0.855 - 0.016b + 0.287b^2 \tag{27}$$

Fig. 12 plots the evolution of the dimensionless parameters characteristic of the experimentally obtained cracks (by fatigue on high-strength steel wires), for the elliptical modelling centred at the cylinder surface (a/b) and for the circular modelling with no restriction (a/R_c).

These relationships may be expresses by fourth-order polynomial expression with a regression coefficient of 0.999 as:

$$\begin{aligned}\frac{a}{b} =& 8.776 - 78.134\frac{a}{D} + 289.984\left(\frac{a}{D}\right)^2 - \\ & - 465.391\left(\frac{a}{D}\right)^3 + 269.108\left(\frac{a}{D}\right)^4\end{aligned} \tag{28}$$

$$\begin{aligned}\frac{a}{R_c} =& 16.296 - 152.026\frac{a}{D} + 557.274\left(\frac{a}{D}\right)^2 - \\ & - 884.522\left(\frac{a}{D}\right)^3 + 507.667\left(\frac{a}{D}\right)^4\end{aligned} \tag{29}$$

Fig. 13 draws the evolution of the crack front shapes in the two modelling procedures on the basis of the real crack fronts experimentally obtained (cf. Fig. 8). It is seen that the two modelling procedures are similar with regard to the crack front

shapes contained in the transverse circular section of the cylinder. It should be emphasized that both methods provide lines (ellipses or circles) contained many points located at the real crack fronts. The value of the error parameter ξ (to evaluate the accuracy of the fitting in both procedures) was very similar in the two methods (Fig. 14), the elliptical one being a little bit more accurate.

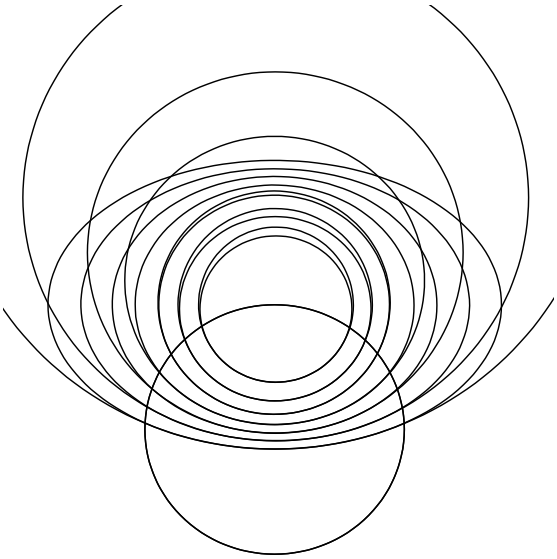

Figure 13: Comparison between the elliptical and the circular fitting

4 Conclusions

A general automated procedure for the geometrical modelling of the surface crack front in cylinders was proposed on the basis of a least squares method and five fitting parameters. It may be simplified to use only three parameters and two symmetric modelling options: an ellipse with its centre located at the cylinder surface and a circle with no restriction regarding the location of its centre.

Both methods were experimentally checked using real crack fronts obtained by fatigue cracking of high-strength steel wires. Both modelling procedures (ellipse and circle) are very adequate, exhibiting a very high accuracy in the modelling of the crack front shapes. The error is always small and decreases for deeper cracks, and the same happens with the differences between both methods. The circular modelling is not adequate in the case of cracks with an aspect ratio a/b higher that one, i.e., cracks in which the depth is higher than the other geometrical dimension.

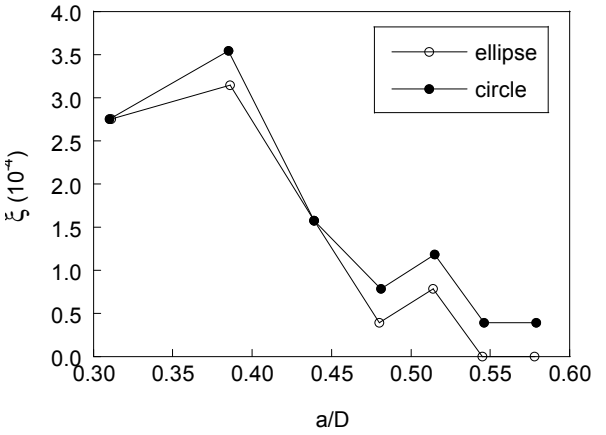

Figure 14: Plot of the ξ parameter as a function of the relative crack depth (a/D) in the two fitting procedures (ellipse and circle)

The dimensionless relationships representing the crack shape evolution in the case of fatigue cracks in high-strength steel wires can me expressed by fourth-order polynomial expression in both modelling procedures. The relationship between the geometrical results in both fitting methods can be expressed by a second-order polynomial expression.

Acknowledgements The authors wish to thank the financial support of their research at the University of Salamanca provided by the following institutions: Spanish Ministry for Education and Science (MEC; Grant BIA2005-08965), Regional Government Junta de Castilla y León (JCYL; Grants SA067A05 and SA111A07), Spanish Foundation "Memoria de D. Samuel Solórzano Barruso" (Grants for Scientific and Technological Research) and University of Salamanca (Grant USAL 2005-09).

References

Carpinteri, A. (1993): Shape change of surface cracks in round bars under cyclic axial loading. *Int J Fract*, vol. 15, pp. 21-26.

Couroneau, N., Royer, R. (2000): Simplifying hypotheses for the fatigue growth analysis of surface cracks in round bars. *Comput Struct*, vol. 77, pp. 381-389.

James, L.A., Mills, W.J. (1988): Review and synthesis of stress intensity factor solutions applicable to cracks in bolts. *Eng Fract Mech*, vol. 30, pp. 641-654.

Levan, A., Royer, J. (1993): Part-circular surface cracks in round bars under ten-

sion bending and twisting. *Int J Fract*, vol. 61, pp. 71-99.

Shin, C.S., Cai, C.Q. (2004): Experimental and finite element analyses on stress intensity factors of an elliptical surface crack in a circular shaft under tension and bending. *Int J Fract*, vol. 129, pp. 239-264.

Toribio, J., Toledano, M. (2000): Fatigue and fracture performance of cold drawn wires for prestressed concrete. *Const Build Mater*, vol. 14, pp. 47-53.